

SIMPLIFIED PREDICTION OF PEAK FLOOR ACCELERATIONS IN INELASTIC WALL STRUCTURES

Lukas Moschen¹, Christoph Adam², and Dimitrios Vamvatsikos³

¹FCP Fritsch, Chiari & Partner ZT GmbH
Marxergasse 1b, 1030 Vienna, Austria
e-mail: moschen@fcp.at

² Department of Engineering Science, University of Innsbruck, Austria
Technikerstr. 13, 6020 Innsbruck, Austria
e-mail: christoph.adam@uibk.ac.at

³ School of Civil Engineering, National Technical University of Athens, Greece
Heroon Polytechniou 9, Athens, Greece
e-mail: divamva@mail.ntua.gr

Keywords: Peak Floor Acceleration, Response Spectrum Method, Inelastic Wall Structures.

Abstract. *In this paper a robust method for simplified prediction of peak floor acceleration (PFA) demands in inelastic structural walls is established. In structural walls the plastic mechanism is usually confined to the domain right above the foundation. It is, thus, reasonable to assume that in wall structures only the response contribution related to the fundamental mode is significantly affected by inelastic deformations. Based on this assumption, a readily developed complete-quadratic-combination (CQC) modal superposition rule for elastic median PFA demand prediction is specialized to inelastic structural walls. In this approach, only the first mode contribution on the PFA demand is affected by inelastic deformations, related to the lateral strength reduction factor identified from the outcomes of a first mode pushover analysis. Since the response contribution of the higher modes is assumed to be elastic, for these modes the relations derived for unlimited elastic structural behavior enter the specialized response spectrum method. Application on a 12-story shear wall shows the accuracy of the predicted median PFA demands derived by the proposed procedure.*

1 INTRODUCTION

Assessment of seismic risk within the performance based earthquake engineering (PBEE) framework requires the prediction of peak floor acceleration (PFA) demands, among other engineering demand parameters. PFA demands are well correlated with damage of acceleration-sensitive nonstructural components (NSCs) [1]. Any response quantity can be estimated by means of nonlinear response history analysis (RHA) yielding “exact” solutions. In engineering practice, however, equivalent static methods are preferred because of low modeling effort, simple application, and low computational costs. FEMA P-58-1 [2], for instance, provides simplified procedures for the assessment of PFA demands (mean and dispersion) of different kinds of structures. Comprehensive summaries of PFA assessment methods are found in [3, 4]. The applicability of the available simplified methods for PFA demand prediction is restricted because of limits on the maximum number of stories, the level of inelasticity, and the irregularity of the considered building. Thus, more robust methods are desirable that can be applied to a larger class of structures, and simultaneously reduce the error relative to the benchmark solution obtained from nonlinear dynamic analysis.

Within the scope of the present contribution a simplified procedure for PFA demand prediction in simple inelastic structures is proposed. The approach combines pushover analysis for predicting the structural strength ratio, and subsequent application of a modified response spectrum method that yields the median PFA demand of the considered structural system [5, 6]. For reasons of simplicity, this novel approach is elaborated for structural walls, where in general the inelastic deformations are confined to the base. The basic idea is that for such simple structures inelastic deformations are solely related to the fundamental mode, and their effect on the response contribution related to the higher modes is small. Thus, the contribution of higher modes on the PFA demand is assumed to be elastic.

Before such a robust simplified method can be established, it is important to understand and reveal the interdependencies of PFA demands on characteristic structural parameters once a structure enters its nonlinear regime of deformation. Thus, in the first part of our contribution the PFA demands of nonlinear single-degree-of-freedom (SDOF) structures are addressed. In a comprehensive parametric study, using sets of earthquake records and nonlinear time history analyses, regression relationships between strength reduction, period, viscous damping, hardening ratio and normalized peak total acceleration demand, i.e., the ratio of inelastic total acceleration to its value at yield, are derived.

These relations are subsequently used to predict the PFA demand related to the fundamental mode of the considered class of inelastic multi-degree-of-freedom (MDOF) structures. The contribution of the first mode inelastic median PFA demand is subsequently superposed with the elastic PFA demands related to the higher modes, using a modified complete-quadratic-combination (CQC) modal superposition rule, originally derived for unlimited elastic structural behavior [5, 6].

Application to a 12-story structural wall shows the accuracy of the predicted inelastic median PFA demands by means of the proposed procedure, when compared to the reference solution based on nonlinear RHA.

2 NORMALIZED PEAK ACCELERATION DEMAND OF NONLINEAR SINGLE-DEGREE-OF-FREEDOM SYSTEMS

Consider an inelastic SDOF system characterized by its initial (elastic) period, T (respectively the natural frequency ω), damping ratio, ζ , yield strength, F_y , strain hardening ratio,

α_{kin} , and the hysteretic material model. The total displacement of the mass, $u(t)$, is the sum of the displacement relative to the support, $u_r(t)$ and the support displacement $u_g(t)$ imposed by the earthquake. In the present study, the considered engineering parameter (EDP), i.e., the peak total acceleration demand, $\max(|\ddot{u}(t)|)$, and the considered intensity measure (IM), i.e., elastic 5 % damped spectral pseudo-acceleration, S_a , are normalized by means of the corresponding quantities at onset of yielding, \ddot{u}_y respectively $S_{a,y}$,

$$\mu_a = \frac{\max(|\ddot{u}(t)|)}{\ddot{u}_y} \quad (1)$$

$$R = \frac{S_a}{S_{a,y}} \quad (2)$$

in which μ_a is the so-called normalized peak (total) acceleration (NPA) demand, and R denotes the *elastic* lateral strength ratio. It should be noted here that, traditionally, the ductility demand of an SDOF system is defined as the ratio of the peak relative displacement to the displacement at the onset of yielding, $\mu = \max(|u_r(t)|)/u_{r,y}$ [7, 8]. The spectral pseudo-acceleration at the onset of yielding, $S_{a,y}$, is related to the spectral yield displacement, $S_{d,y}$, as [9]

$$S_{a,y} = \omega^2 S_{d,y} \quad (3)$$

Subsequently, a relationship between NPA demand μ_a , R -factor and period T of non-degrading SDOF systems with bilinear or peak-oriented (Clough model [10]) behavior subjected to a set of ground motion record is derived. The proposed relation is found by repeated RHA varying period T and the R -factor of the SDOF oscillator subjected the ground motions of the considered sets discussed later on. Since P-delta effects are neglected, this analysis is equivalent to incremental dynamic analysis (IDA) [11].

2.1 Characteristic parameter dependences of the normalized peak acceleration demand

At first, as an example the effect of damping on the NPA demand is studied on perfectly plastic ($\alpha_{kin} = 0$) bilinear SDOF oscillators with period $T = 1.0$ s. The oscillators are subjected to the 44 records of the FEMA P695 far-field ground motion set [12], referred to as FEMA P695-FF set. The FEMA P695-FF records include seismic events of magnitude M_w between 6.5 and 7.6, and closest distance to the fault rupture larger than 10 km. The Joyner-Boore distance is between 7.1 and 26 km. Only strike-slip and reverse sources are considered. The 44 records of this set were recorded on NEHRP site classes C (soft rock) and D (stiff soil). Detailed information is provided in [12].

IDAs yield the $R - \mu_a$ relations shown in Figure 1 for four differently damped systems with damping ratios $\zeta = 0\%$, 1% , 5% and 10% . Gray lines represent the 44 single record IDA curves, and the corresponding median, the 16 % and 84 % quantiles are shown by black lines. The dash-dotted line represents the $R - \mu_a$ relation of the equivalent linear system.

Clearly, the inelastic NPA demand is always smaller than the corresponding elastic one. In the elastic deformation range, i.e., $R \leq 1$, the NPA demand and the R -factor are identical, yielding a record and damping independent $R - \mu_a$ relation. For zero damping, the spectral pseudo-acceleration S_a corresponds to the total acceleration, and thus, in the complete inelastic deformation branch (i.e., $R > 1$) the NPA demand is one, as depicted in Figure 1a. For non-zero damped systems, the difference between the spectral pseudo-acceleration S_a and the total acceleration results in the inelastic range in a more or less *linear* increase of the NPA demand with increasing R -factor, compare with Figures 1b to 1d. It is furthermore observed that the

slope of the median normalized acceleration demand $\check{m}_a \equiv \mu_{a,50\%}$ (with respect to the straight vertical line at $\mu_a = 1$ in Figure 1) increases by the same factor as the damping ratio becomes larger; compare the median in Figure 1c with the median in Figure 1d. That is, for instance, the ratio of $\mu_{a,50\%}$ given $R = 6$ for $\zeta = 0.10$ and $\zeta = 0.05$ can be approximated as

$$\frac{\mu_{a,50\%,\zeta=0.05} - 1}{\mu_{a,50\%,\zeta=0.10} - 1} \approx \frac{\zeta = 0.10}{\zeta = 0.05} = 2 \quad (4)$$

Thus, assuming that for a reference damping ratio ζ^* the $R - \mu_{a,50\%,\zeta^*}$ relation is available, for other damping ratios ζ this relation can be approximately expressed according to

$$\mu_{a,50\%,\zeta} = 1 + \frac{\zeta^*}{\zeta} (\mu_{a,50\%,\zeta^*} - 1) \quad (5)$$

This relation not only holds for bilinear systems but also for non-degrading oscillators with other cyclic behavior. As an example, Figure 2b shows for the 1.0 s 5% damped oscillator *but* with assigned peak-oriented hysteretic loop the IDA curves, which are almost identical with the ones of the bilinear counterpart system, compare with Figure 1c.

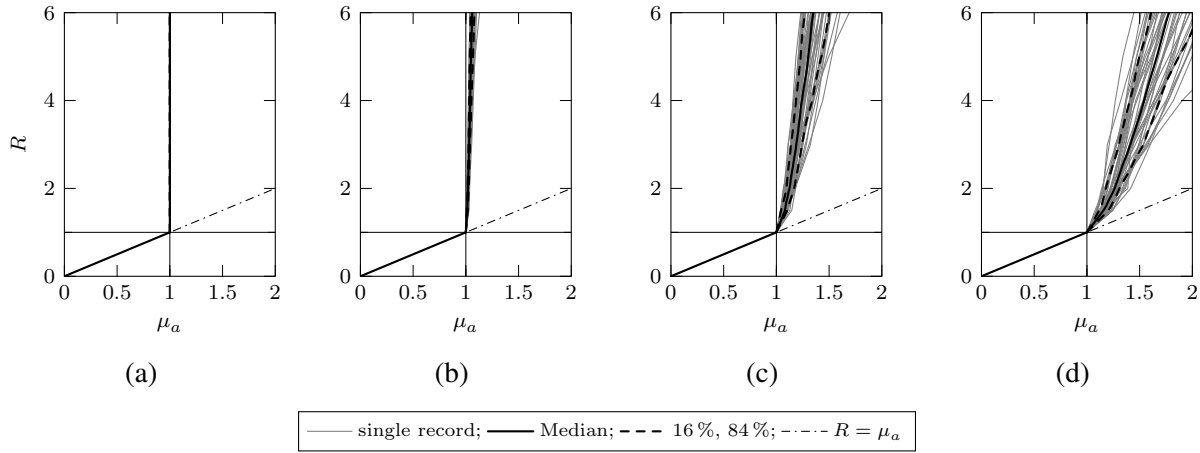


Figure 1: R -factor with respect to normalized peak acceleration demand μ_a of perfectly plastic bilinear ($a_{kin} = 0$) $T = 1.0$ s oscillator subjected to the 44 records of the FEMA P695-FF record set. For different damping ratios: (a) $\zeta = 0$, (b) $\zeta = 0.01$, (c) $\zeta = 0.05$, and (d) $\zeta = 0.10$.

In similar fashion, Moschen [3] varied the strain hardening coefficient, a_{kin} , in the range $0 \leq a_{kin} \leq 0.05$, and he found again in the post-yield range a virtually linear relationship between R and $\mu_{a,50\%,a_{kin}}$ with a slope proportional to the actual value of a_{kin} , compare, for instance, Figure 1c with Figure 2a, and Figure 2b with Figure 2c. Consequently, with known $R - \mu_a$ relation for reference hardening ratio a_{kin}^* , the median NPA demand can be approximated in analogy to Equation (5) as

$$\mu_{a,50\%,a_{kin}} = 1 + \frac{a_{kin}^*}{a_{kin}} (\mu_{a,50\%,a_{kin}^*} - 1) \quad (6)$$

Equations (5) and (6) consider the effect of damping ratio and hardening coefficient on the NPA demand separately. Thus, in the next step, Equations (5) and (6) are combined to express the $R - \mu_{a,50\%}$ relation as a function of both a_{kin} and ζ ,

$$\mu_{a,50\%} = p \left(1 + \frac{\zeta^*}{\zeta} (\mu_{a,50\%}^* - 1) \right) + (1 - p) \left(1 + \frac{a_{kin}^*}{a_{kin}} (\mu_{a,50\%}^* - 1) \right) \quad (7)$$

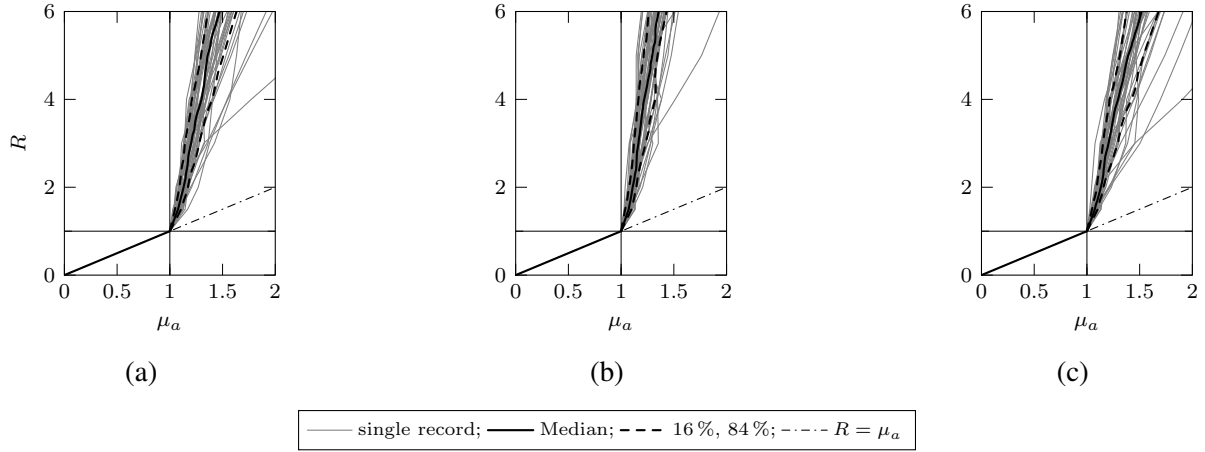


Figure 2: Impact of different material models on the IDA curves of the $\zeta = 0.05$ mass proportional damped SDOF oscillator with period $T = 1.0$ s in $R - \mu_a$ coordinates. (a) Bilinear hysteretic material with hardening coefficient $a_{kin} = 0.05$, peak-oriented hysteretic material with (b) $a_{kin} = 0$, and (c) $a_{kin} = 0.05$.

with $\mu_{a,50\%}^* \equiv \mu_{a,50\%,a_{kin}^*,\zeta^*}$ denoting the *base case* NPA demand for reference damping coefficient ζ^* and reference hardening ratio a_{kin}^* . Since both damping and hardening ratio affect the $R - \mu_a$ relation in the same order, factor p is approximated as $p = 1/2$.

From now on reference damping ratio is set to $\zeta^* = 0.05$, and reference hardening ratio to $a_{kin}^* = 0.05$.

For all $R - \mu_a$ relations, regardless of damping type, damping ratio, and nonlinear material properties, the presented relations can be used until the structure has been pushed to the ultimate lateral strength reduction factor,

$$R_{ult} = \frac{S_{a,ult}}{S_{a,y}} \quad (8)$$

in which $S_{a,ult}$ is the ultimate spectral pseudo-acceleration defined by the capping strength of the backbone curve of the material model if P-delta effects are *not* considered. This study, however, focuses on SDOF systems (a) with non-degrading material properties, and (b) nonlinear geometric transformations are neglected. This implies infinite ultimate capacity, $S_{a,ult} \rightarrow \infty$.

2.2 Normalized peak acceleration demand for the FEMA P695-FF record set

By now, the $R - \mu_a$ relation has been discussed for period $T = 1.0$ s only. Repeating the analysis for a series of periods in the range of 0.1 s to 3.2 s and reference parameters $a_{kin}^* = 0.05$ and $\zeta^* = 0.05$ results in the median $R - \mu_a - T$ relation of the nonlinear base-case SDOF oscillator shown in Figure 3a for $R > 1$.

To derive more convenient analytical approximations, here the outcomes are shown in terms of EDP-IM coordinates, in contrast to the traditional representation in IM-EDP coordinates [11]. Thus, in the contour plot depicted in Figure 3b the contour lines correspond to curves of constant $\mu_{a,50\%,a_{kin}^*,\zeta^*}$ values (in contrast to the study of [7], where surface plots for R -factors were used).

Inspection of Figure 3a leads to the conclusion that the $R - \mu_{a,50\%,a_{kin}^*,\zeta^*}$ relation is virtually

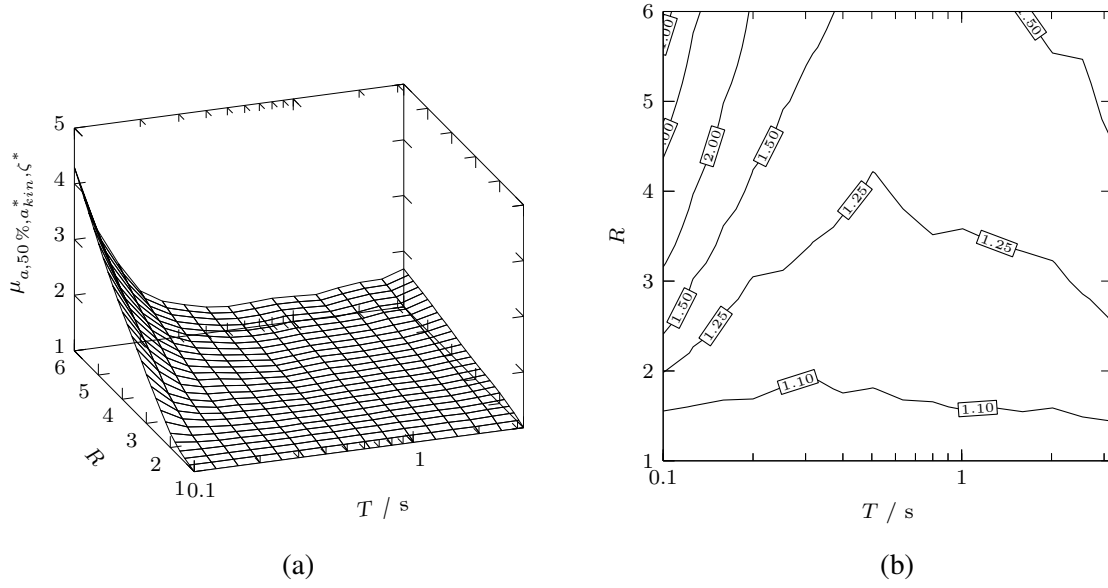


Figure 3: Median normalized peak acceleration demand $\mu_{a,50\%}^*$ with respect to period T and R -factor for base case SDOF system subjected to the FEMA P695-FF record set. (a) Surface plot. (b) Contour plot.

linear regardless of the period. The corresponding linear approximation, $\tilde{\mu}_{a,50\%}$, reads as

$$\mu_{a,50\%}^* \approx \tilde{\mu}_{a,50\%}^* = \begin{cases} 1 & \text{for } R \leq 1 \\ c(R - 1) + 1 & \text{for } R > 1 \end{cases} \quad (9)$$

in which unknown coefficient c represents the slope of $\tilde{\mu}_{a,50\%}^*$. This coefficient depends on period T and is in the range $0 \leq c < 1$. At very short periods, slope c of $\mu_{a,50\%}^*$ is steepest, as seen from Figure 3.

Equation (9) is the basis of a two-stage fit, using the Levenberg-Marquardt algorithm at each stage, which is implemented in the curve fitting toolbox of Matlab [13]. In the first stage, the approximation $\tilde{\mu}_{a,50\%}^*$ (Equation (9)) is fitted to the empirical data, $\mu_{a,50\%}^*$, for each individual period separately. Since in Equation (9) the only unknown parameter is c , to each period an individual parameter c is mapped, graphically shown by circular markers in Figure 4. Stage two fits a function \tilde{c} to the discrete parameters c , yielding the two-term exponential equation

$$c \approx \tilde{c} = \beta_1 e^{\beta_2 T} + \beta_3 e^{\beta_4 T}, \quad 0 \leq c < 1 \quad (10)$$

In Table 1 coefficients $\beta_1, \beta_2, \beta_3, \beta_4$ and the corresponding 95 % confidential interval (median $\pm 2\sigma$) are listed. The 2σ bounds represent the 5 % confidence limits of a standardized normal distributed random variable, which is, for instance, appropriate for the sample mean. Therefore, it can be used for model validation (equivalent to the χ^2 -test) in an effort to make a decision if the analytical model should be accepted or rejected. For detailed information regarding hypothesis testing and model validation the reader is referred to [14].

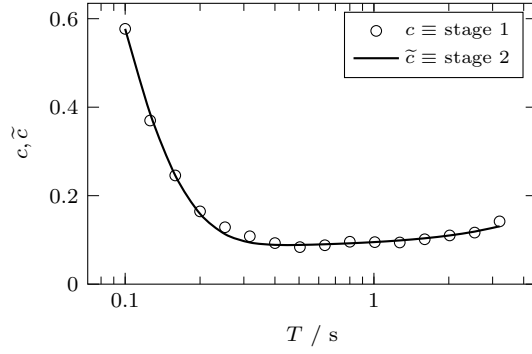


Figure 4: Two-stage fit of slope \tilde{c} based on the FEMA P695-FF record set.

Table 1: Coefficients β_1 to β_4 and their 95 % confidence bounds for slope \tilde{c} based on the FEMA P695-FF record set.

i	β_i	$\beta_i - 2\sigma$	$\beta_i + 2\sigma$
1	1.09	1.07	1.12
2	-20.29	-21.01	-19.57
3	0.07	0.06	0.07
4	0.18	0.16	0.20

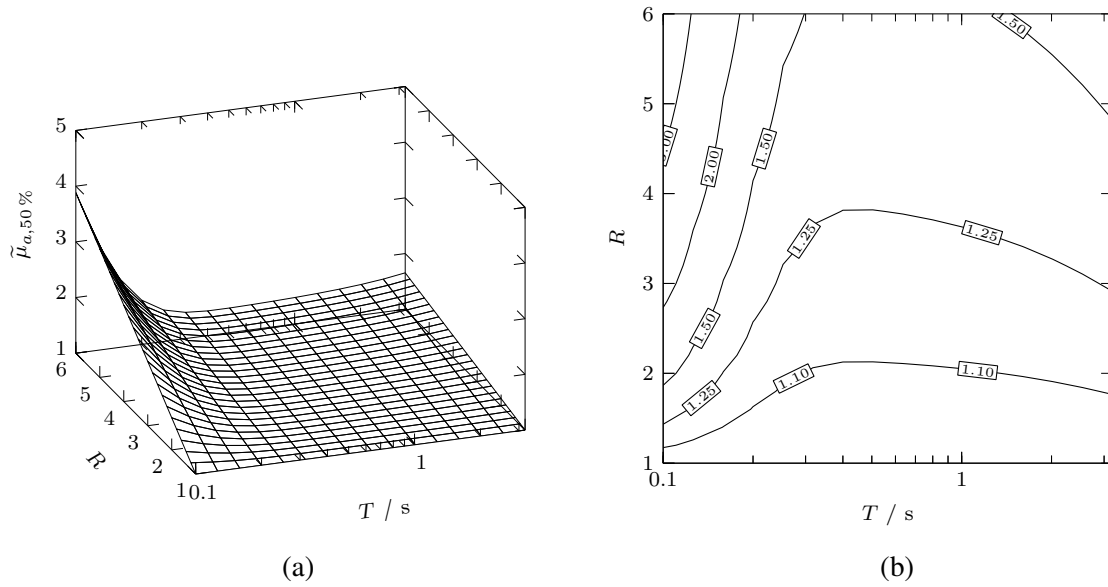


Figure 5: Design median normalized peak acceleration demand $\tilde{\mu}_{a,50\%}^*$ with respect to period T and R -factor for base case SDOF system subjected to the FEMA P695-FF record set. (a) Surface plot. (b) Contour plot.

The median NPA demand $\tilde{\mu}_{a,50\%}$ for damping coefficient and/or hardening ratio different from the base case values is found from Equation (7).

2.3 Normalized peak acceleration demand for the Century City record set

Alternatively, an analytical relation for the parameter dependent NPA demand is determined for the Century City record set [15], which consists of 92 ground motions of the PEER ground motion database [16]. These records have been selected using a multi-objective optimization procedure by minimizing two fitness functions. The advantage is that this record set matches the design response spectrum *and* a constant dispersion spectrum of Century City relatively well over a wide period region. Therefore, a broad class of buildings located in Century City can be assessed (or designed, respectively) by this record set without conducting record selection with respect to the fundamental period of every individual structure separately. This record selection procedure can be seen as an alternative to the existing body of conditional mean spectrum (CMS) methods [17, 18]. Figure 6 shows the target spectra (bold black lines), the 92 individual

response spectra (gray lines), and the corresponding statistical quantities (thin black lines) of the Century record set, which will be used for analyses in the remainder of this paper. For detailed information of the record selection procedure the reader is referred to [15, 3].

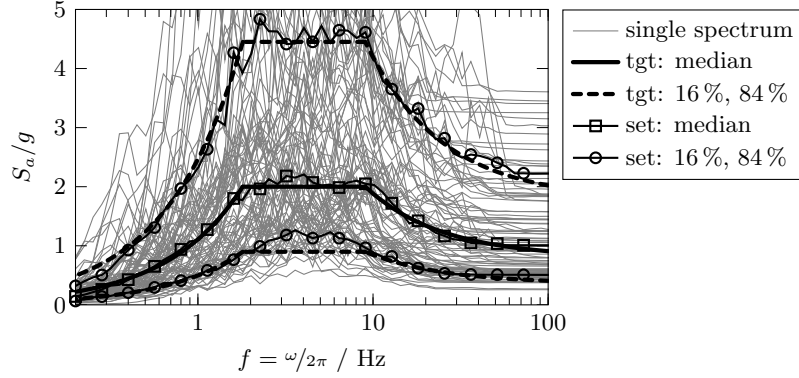


Figure 6: Century City records set: Target response spectra (bold black lines), response spectra of individual records (gray lines), and statistical quantities (lines with markers) for a normal target dispersion $\sigma_t = 0.80$ [5, 6, 15].

The same procedure as detailed for the FEMA P695-FF record set yields coefficient c as a function of T shown in Figure 7 with circular markers (individual c -values as outcome of the fitting first stage) and the black solid line (functional relation resulting from the second stage). Table 2 lists the corresponding coefficients for evaluation of Equation (10).

As observed, the two-stage fit of c , and consequently, the $R - \tilde{\mu}_{a,50\%}^* - T$ relation is for both record sets in good agreement, because median spectral shapes and the corner frequencies of the sets are similar.

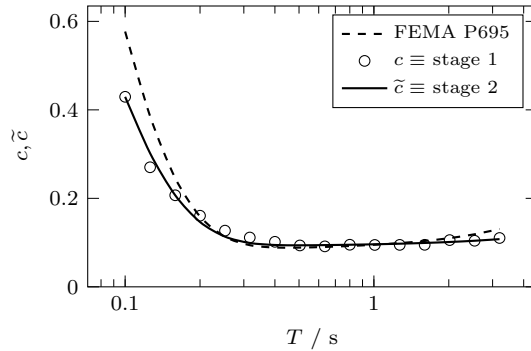


Figure 7: Two-stage fit of slope \tilde{c} based on the Century City record set.

Table 2: Coefficients β_1 to β_4 and their 95 % confidence bounds for slope \tilde{c} based on the Century City record set.

i	β_i	$\beta_i - 2\sigma$	$\beta_i + 2\sigma$
1	2.10	1.64	2.56
2	-18.27	-20.33	-16.22
3	0.09	0.08	0.10
4	0.05	0.00	0.11

3 RESPONSE SPECTRUM METHOD FOR PEAK FLOOR ACCELERATION DEMANDS IN INELASTIC WALL STRUCTURES

3.1 Approximate peak floor acceleration demand prediction in elastic structures

One ingredient of the proposed simplified PFA demand prediction of inelastic shear walls is a modified form of a CQC modal superposition rule for elastic structures, which was more recently presented in [1, 5, 19]. Accordingly, the elastic median PFA demand of the k th degrees-

of-freedom of an N DOF structure can be estimated as

$$pfa_k = \left[\sum_{i=1}^n \sum_{j=1}^n \left(\frac{p_k}{p_i} \right) \left(\frac{p_k}{p_j} \right) \phi_{i,k} \Gamma_i S_{a,i} \phi_{j,k} \Gamma_j S_{a,j} \rho_{i,j} + \left(\frac{p_k}{p_g} \right)^2 pga^2 r_{n,k}^2 + 2pga r_{n,k} \left(\frac{p_k}{p_g} \right) \sum_{i=1}^n \left(\frac{p_k}{p_i} \right) \phi_{i,k} \Gamma_i S_{a,i} \rho_{i,g} \right]^{\frac{1}{2}} \quad (11)$$

in which variables ϕ_i , Γ_i , $S_{a,i}$, and p_i denote the i th mode shape, participation factor, spectral pseudo-acceleration and modal peak factor, respectively. Subscript g denotes the corresponding quantities of the ground acceleration; the spectral pseudo-acceleration of the ground degenerates to the peak ground acceleration, pga . Variable $\rho_{i,j}$ represents the correlation coefficient between the i th and the j th modal total acceleration, and $\rho_{i,g}$ the correlation coefficient between the i th modal total acceleration and the ground acceleration. The peak factor of the response process of the k th degree of freedom is denoted by p_k . To reduce the computational effort, in the response analysis only the first n modes are considered. The truncation error arising from disregarding the $(n+1)$ th to N th mode is reduced through residual vector \mathbf{r}_n , with its k th element [5]

$$r_{n,k} = 1 - \sum_{i=1}^n \phi_{i,k} \Gamma_i \quad (12)$$

3.2 Approximate peak floor acceleration demand prediction in inelastic wall structures

Subsequently, a first mode approximation for predicting inelastic PFA demands presented in [20] is extended in an effort to consider also higher modes.

Consider an inelastic MDOF structure, where the plastic mechanism is mainly governed by the fundamental mode. An example of such simple nonlinear MDOF systems is the family of *regular structural walls* that have in common that the plastic zones are confined to the base [21]. It is reasonable to assume that in those structures the portion of the PFA demand related to the fundamental mode shows a similar performance as inelastic SDOF systems. Thus, this part of the PFA demand can be determined based on the relations present in the previous section for inelastic SDOF systems. On the other hand, the PFA demand associated with the higher modes is assumed to be unlimited elastic, and thus, this portion is determined in analogy to modal superposition for elastic systems according to Equation (11). The proposed procedure involves the steps as outlined below.

Structural modeling In the first step a structural model of the considered structural wall is created. In many cases, an equivalent stick model with a nonlinear rotational spring at the base, such as shown in Figure 8a, represents appropriately the wall. Spring parameters $c_{\theta 0}$, M_{y0} and α_s denote the rotation at the onset of yielding, the corresponding yield strength, and the hardening ratio, respectively.

Modal analysis Modal analysis yields the periods and corresponding mode shapes of the structural model.

Pushover analysis A first mode pushover analysis is conducted to identify the plastic mechanism. From the global pushover curve the R -factor and the global hardening ratio a_{kin} are identified, as shown exemplary in Figure 9b for different R -factors. For a structural

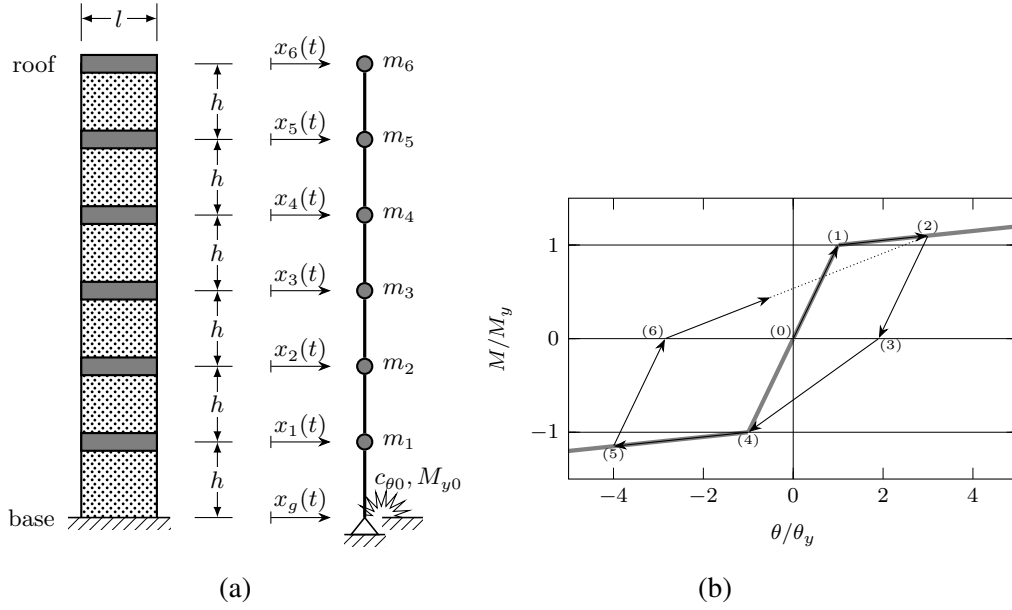


Figure 8: (a) Planar structural wall and the corresponding stick model with nonlinear rotational spring at the base, and (b) Clough material model assigned to the nonlinear rotational spring at the base.

model with a nonlinear spring at the base, the transition between elastic and inelastic deformation branch is discontinuous with a kink at the yield displacement. Transformation of the pushover curve into IM-EDP coordinates of the equivalent SDOF-domain is not necessary, because the R -factor and a_{kin} can be directly read from the pushover curve.

NPA demand related to the fundamental mode With available fundamental period T_1 (utilized instead of SDOF system period T), R -factor and global hardening ratio a_{kin} , subsequent evaluation of Equation (9) and Equation (7) yields an estimate of the median NPA demand associated with the fundamental mode, $\mu_{a,50\%}^{(1)}$. Dividing the elastic 5% damped median spectral pseudo-acceleration at period T_1 , $S_{a,1} \equiv S_a(T_1)$, by the R -factor, results in the median spectral pseudo-acceleration at onset of yielding, $S_{a,y}(T_1) = S_{a,1}/R$, compare with Equation (2). Substituting $S_{a,y}(T_1)$ for total median acceleration of the fundamental mode at onset of yield $\ddot{u}_y^{(1)}$, i.e., $\ddot{u}_y^{(1)} \approx S_{a,y}(T_1)$, and multiplying this quantity by $\mu_{a,50\%}^{(1)}$, yields an estimate of the first mode peak acceleration demand, i.e., $\max |\ddot{u}_{50\%}^{(1)}| = \mu_{a,50\%}^{(1)} \ddot{u}_y^{(1)}$, compare with Equation (1).

CQC modal superposition modified for inelastic structures The proposed modal superposition method PFA prediction in inelastic structures is based on a modification of the CQC method of Equation (11) for elastic systems. In particular, the elastic 5% spectral pseudo-acceleration $S_{a,i}$ (respectively $S_{a,j}$) is replaced by $\bar{S}_{a,i}$, where $S_{a,1}$ is approximated by the first mode total peak acceleration demand $\max |\ddot{u}_{50\%}^{(1)}|$, i.e., $\bar{S}_{a,1} \approx \max |\ddot{u}_{50\%}^{(1)}|$, and for the higher modes the elastic spectral pseudo-acceleration is utilized, i.e., $\bar{S}_{a,i} = S_{a,i}$.

Furthermore, the median peak factor p_1 related to the fundamental mode must be modified when considering inelastic deformations. Figure 1a shows that for non-hardening SDOF oscillators the yield acceleration and the peak acceleration are equal, and the standard

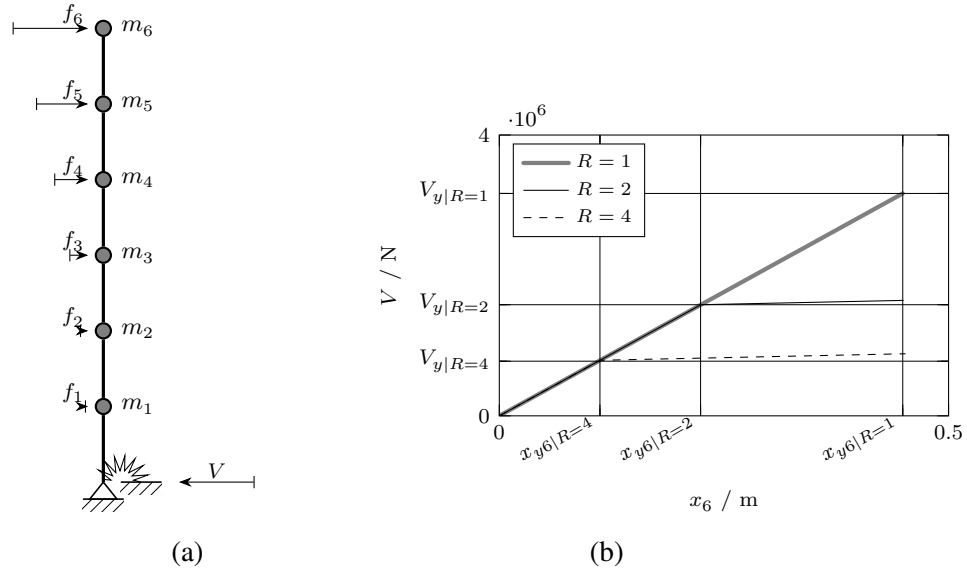


Figure 9: (a) Stick model with load pattern consistent with fundamental mode, and (b) pushover curves evaluated for different lateral strength ratios.

deviation of this quantity is zero. Therefore, the peak factor, which represents the ratio between the peak acceleration and the mean square acceleration of a normal stationary random process [5, 6], is unity, i.e. $p_i = 1$. Preliminary studies have shown that this relation can also be applied for structures with moderate hardening backbone curve. The modal peak factors of the higher (elastic) modes, $p_i, i > 1$, and the peak factor of the response process, p_r , can be estimated by the framework for elastic structures provided in [5, 6], as preliminary studies have shown.

3.3 Application

The proposed modified CQC method for median PFA prediction in inelastic shear walls is tested on the example of a 12-story regular generic structural wall, with a fundamental period tuned to the value specified in ASCE 7-10 [22] ($T_1 = 0.83$ s), a parabolic fundamental mode shape, and a pre-defined lateral strength ratio R . The details on mass, stiffness, and strength properties can be found in [3]. The structure is assumed to be located in Century City (Los Angeles, CA; 34.053 66° N, 118.413 39° W), and thus, empirical relation Equation (10) based on the Century City record set is used for the subsequent PFA assessment.

The results of the proposed modal superposition procedure are validated with the outcomes of nonlinear RHA using the 92 ground motions of the Century City record set. Thus, a hysteretic relation between load cycles must be specified. In the present study, in the framework of the lumped plasticity approach to the base spring the Clough material model [10] (a uniaxial material model with peak oriented hysteresis and infinite ductility), shown in Figure 8b, is assigned. This constitutive relation allows to account for reloading stiffness degradation once the yield strength has been exceeded (compare with the reduced reloading stiffness between points (6) and (2)).

Figure 10 depicts the profiles of the median PFA demand of the 12-story structural wall for lateral strength ratios $R = 1, 2, 4, 6$ (columns 1 to 4). Rows 1 to 3 show the reference solutions obtained from RHA (solid gray lines), their approximations by the proposed CQC modal combination rule (solid black line), and the common square-root-of-the-sum-of-the-squares (SRSS)

rule (dashed black line) based on a fundamental mode approximation (row 1), a two-mode approximation (row 2), and considering all modes up to the 95 % cumulative mass participating mode (row 3).

The reference solutions for various R -factors reveal that the PFA demands saturate once the structure starts yielding. This outcome is consistent with findings reported in [23, 24]. In other words, it can be concluded that with increasing ground motion intensity the related increase of the median PFA demand is quite low when the yield strength is exceeded. This observation is consistent with the results previously shown for nonlinear SDOF oscillators. Since for this 12-story structural wall the plastic deformations are concentrated at the base, the elastic PFA demand related to the higher modes contribute to the total PFA demand in the same order regardless of the lateral strength ratio.

Subsequently, the PFA demands obtained by the proposed CQC modal combination rule are discussed in more detail. It is observed that a fundamental mode approximation (first row) does not approximate appropriately the actual PFA demand. The nonlinearity of the corresponding median PFA profile is the result of the correlation between modal total acceleration and ground acceleration, and the corresponding peak factors according to the second and the third term of Equation (11) [5]. The median PFA profile based on a two-modes approximates closely the reference solution, as shown in the second row of Figure 10. Consideration of the modes up to the 95 % cumulative mass participating mode yields an excellent approximation of the median PFA demand regardless of the lateral strength ratio.

Additionally, the outcomes of the SRSS approach, commonly used in engineering practice due to its simplicity, are also presented. Equation (11) degenerates to the SRSS rule when dropping the second and the third term of this equation, as well as the peak factors and the modal correlation (i.e. $i = j$). Consequently, the SRSS first mode approximation of the median PFA profile is affine to the fundamental mode shape, which is in the considered example parabolic, compare with the dashed lines in the first row of Figure 10. The SRSS rule was developed to estimate relative response quantities, such as displacements and internal forces, and thus, this approach underestimates the peak total acceleration demand since the contribution of the PGA demand is not considered. However, a multi-modal SRSS approximation of the median PFA demand yields for the upper floors reasonable predictions of this response quantity, because the effect of the PGA diminishes with increasing height, see the dashed graphs in the third row of Figure 10. It should be noted here that the SRSS modal combination rule is deemed to fail for estimating PFA demands in spatial structures, because closely spaced modes are neglected [5, 6].

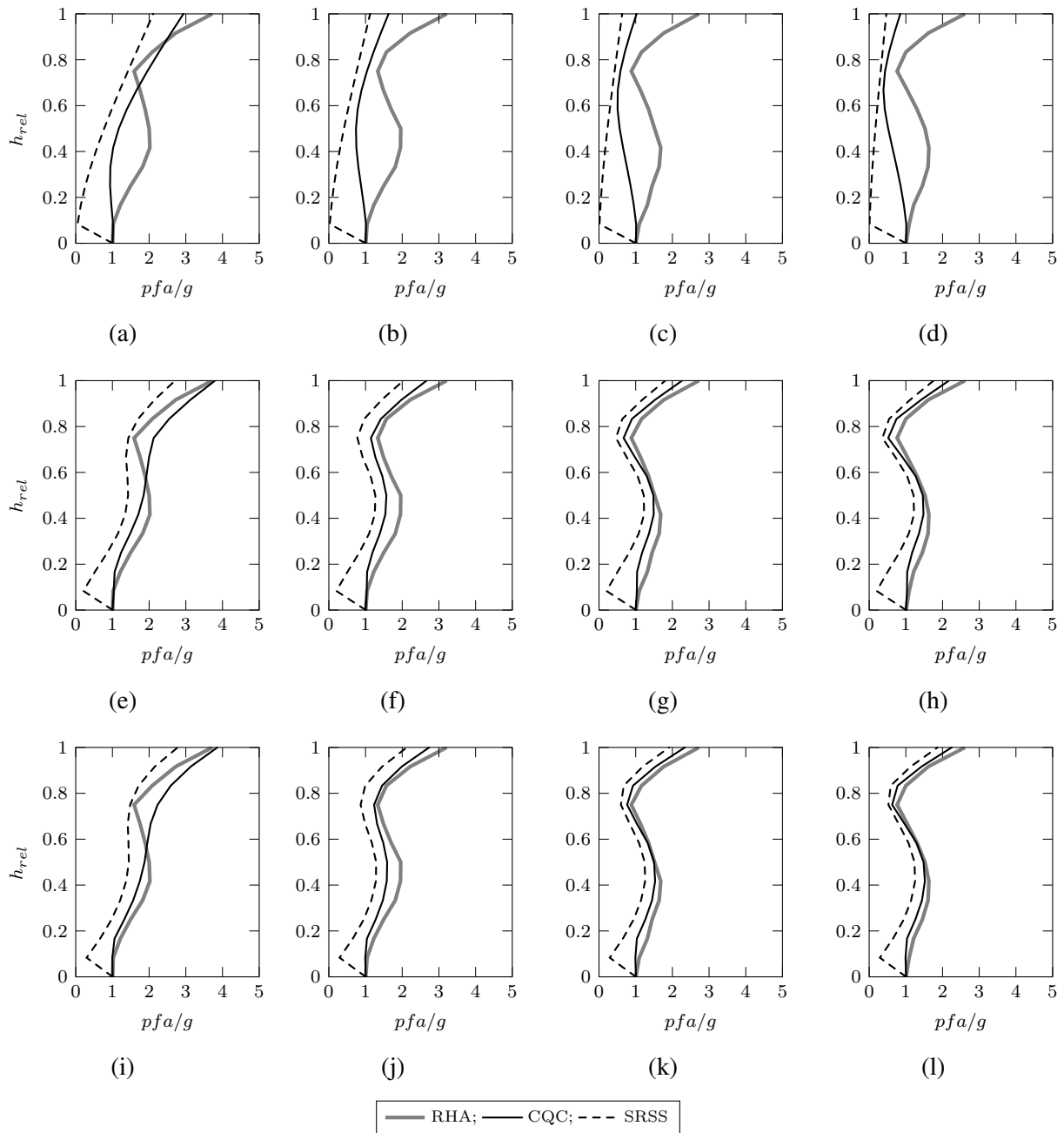


Figure 10: Profiles of the median PFA demand for the 12-story structural wall. Reference solution based on RHA (gray lines), the proposed CQC modal combination rule (black solid lines) and the SRSS approximation (dashed black lines). Results presented for lateral strength ratios $R = 1, 2, 4, 6$ (columns 1 to 4) considering one mode (first line), two modes (second line), and 95 % cumulative mass participating modes (third line).

4 CONCLUSION

In this contribution a simple but effective procedure for estimating the median peak floor acceleration (PFA) demands in inelastic planar wall structures has been presented, based on readily available concepts, such as pushover analysis and modal combination.

The fundamental idea of this procedure is that for certain MDOF structures such as shear walls the inelastic PFA demand is primarily related to the fundamental mode, while the contribution of the higher modes on this response quantity remains mainly unaffected by plastic deformations. In the considered class of MDOF structures the lateral strength ratio can be estimated by nonlinear static procedures, which allows to estimate a reduced spectral PFA demand associated with the fundamental mode by means of the concept of normalized peak acceleration (NPA) demand for nonlinear SDOF oscillators derived in the first part of this study. Then, the reduced spectral peak acceleration demand for this mode enters a modified CQC rule developed originally for *elastic* PFA demands. Application to an inelastic 12-story shear wall shows that this simple procedure yields an excellent approximation of the median PFA demands regardless of lateral strength ratio.

Because of the simplicity of the proposed framework a clear physical interpretation of PFA demand prediction becomes possible. This procedure may serve as alternative for codified PFA assessment methods, which yield in general only a rough prediction of this response quantity.

REFERENCES

- [1] S. Taghavi, E. Miranda, Response spectrum method for estimation of peak floor acceleration demands. *Proceedings of the 14th World Conference on Earthquake Engineering (14WCEE)*, Beijing, China, October 12-17, 2008.
- [2] FEMA P-58-1, *Seismic Performance assessment of buildings, Volume 1 – Methodology*, Washington, DC, 2012.
- [3] L. Moschen, Contributions to the probabilistic seismic assessment of acceleration demands in buildings. *Dissertation, Unit of Applied Mechanics, University of Innsbruck*, 2016.
- [4] V. Vukobratović, The influence of nonlinear seismic response of structures on the floor acceleration spectra. *Dissertation, Faculty of Civil and Geodetic Engineering, University of Ljubljana*, 2015.
- [5] L. Moschen, C. Adam, D. Vamvatsikos, A response spectrum method for peak floor acceleration demands in earthquake excited structures. *Probabilistic Engineering Mechanics*, **46**, 94–106, 2016.
- [6] L. Moschen, C. Adam, Peak floor acceleration demand prediction based on response spectrum analysis of various sophistication. *Acta Mechanica*, DOI: 10.1007/s00707-016-1756-5.
- [7] E. Miranda, V.V. Bertero, Evaluation of strength reduction factors for earthquake-resistant design. *Earthquake Spectra*, **10**, 357–379, 1994.
- [8] T. Vidic, P. Fajfar, M. Fischinger, Consistent inelastic design spectra: strength and displacement. *Earthquake Engineering & Structural Dynamics*, **23**, 507–521, 1994.

- [9] A.K. Chopra, Dynamics of Structures. 4th ed. *Prentice Hall*, 2012.
- [10] R.W. Clough, Effect of stiffness degradation on earthquake ductile requirements. *Structures and Materials Research Research Department of Civil Engineering*, UCB/SESM Report 66-16, University of California at Berkeley, 1966.
- [11] D. Vamvatsikos, C.A. Cornell, Incremental dynamics analysis. *Earthquake Engineering & Structural Dynamics*, **31**, 491–514, 2002.
- [12] FEMA P695, *Quantification of building seismic performance factors*, Washington, DC, 2009.
- [13] Matlab, *The MathWorks Inc.*, 2016.
- [14] J.R. Benjamin, C.A. Cornell, Probability, Statistics, and Decision for Civil Engineers. *Dover Books on Engineering*, *Dover Publications*, 1970.
- [15] L. Moschen, R.A. Medina, C. Adam, A ground motion record selection approach based on multi-objective optimization. Accepted for publication in: *Journal of Earthquake Engineering*.
- [16] Pacific Earthquake Engineering Research Center, *PEER Ground Motion Database*, University of California at Berkeley, 2010.
- [17] N. Jayaram, T. Lin, J.W. Baker, A computationally efficient ground-motion selection algorithm for matching a target response, Spectrum Mean and Variance. *Earthquake Spectra*, **27**, 797–815, 2011.
- [18] J.W. Baker, Conditional mean spectrum: tool for ground-motion selection. *Journal of Structural Engineering*, **137**, 322–331, 2011.
- [19] M. Pozzi, A. Der Kiureghian, Response Spectrum analysis for floor acceleration. *Earthquake Engineering & Structural Dynamics*, **44**, 2111–2127, 2015.
- [20] L. Moschen, D. Vamvatsikos, C. Adam, Towards a static pushover approximation of peak floor accelerations. *Vienna Congress on Recent Advances in Earthquake Engineering and Structural Dynamics 2013 (VEESD 2013)*, Vienna, Austria, August 28-30, 2013.
- [21] L. E. Garcia, M.A. Sozen, Earthquake-resistant design of reinforced concrete buildings. *From Engineering Seismology to Performance-Based Engineering*, Chapter 14, 2004.
- [22] ASCE/SEI 7-10, Minimum design loads for buildings and other structures. *American Society of Civil Engineers/Structural Engineering Institute*, 2010.
- [23] E. Miranda, S. Taghavi, A comprehensive study of floor acceleration demands in multi-story buildings. *ATC and SEI Conference on Improving the Seismic Performance of Existing Buildings and Other Structures*, San Francisco, California, December 9-11, 2009.
- [24] R. Sankaranarayanan, R.A. Medina, Acceleration response modification factors for non-structural components attached to inelastic moment-resisting frame structures. *Earthquake Engineering & Structural Dynamics*, **36**, 2189–2210, 2007.